JOURNAL OF SPACECRAFT AND ROCKETS
Vol. 43, No. 5, September–October 2006

Role of Water Vapor in Solar Array Arc Initiation: Dissociative Recombination Processes

Joel T. Galofaro*
NASA John H. Glenn Research Center at Lewis Field, Cleveland, Ohio 44135
Boris V. Vayner†
Ohio Aerospace Institute, Cleveland, Ohio 44192
Wilhelmus A. Degroot‡
Silicon Light, Inc., Sunnyvale, California 94087
and
Dale C. Ferguson§
NASA Marshall Space Flight Center, Huntsville, Alabama 35812

DOI: 10.2514/1.21639

Strong supporting evidence that adsorbed water vapor residing at the triple junction sites on a solar array is a leading contributing factor to arcing onset in conventional silicon photovoltaic arrays immersed in low Earth orbital plasmas is presented. It is suggested that an adsorbed water vapor layer becomes ionized by energetic electrons and that the discharge develops in the area of a triple junction. The fastest process to extinguish the discharge is the dissociative recombination of water molecular ions. Arc plasma spectroscopic data throughout the wavelength range 260–680 nm is obtained. The two most intensive silver lines in the UV spectrum (Ag I, 328 and 338 nm), an atomic silver line (Ag I, 358.6 nm), and two lines of singly ionized silver atoms (Ag II, 318.7 and 368.2 nm) are identified. Additionally, atomic line spectra Fe I (415.87 nm) and Ni I (480.7 nm) are found. More importantly, identification of several species that appear to validate a dissociative recombination process involving water vapor is also found. The observations involved are the OH molecular band (302–309 nm) and two intensive atomic lines (H-α, 656.3 nm, and H-β, 486 nm). The following species with molecular bands, CH (432 nm), SiH (387 nm), and SiN (472 nm) are also identified.

Nomenclature

A	=	molecular mass
C	=	capacitance, μF
e	=	electron charge, C
k	=	Boltzmann constant, ergs [eV]$^{-1}$
I	=	current, A
m_p	=	proton mass, g
N_i	=	total number of metal ions
N_W	=	total number of adsorbed molecules
n_e	=	electron number density, cm^{-3}
P	=	pixel number
R	=	radius of sphere, cm
$\Re$	=	recombination rate, s$^{-1}\cdot$cm^{-3}
S	=	area, cm^2
T_e	=	electron temperature, eV
t	=	time, s
U	=	bias voltage, V
V_e	=	electron velocity, cm $\cdot$ s^{-1}
γ	=	recombination constant, cm$^3\cdot$s^{-1}
Δq	=	electrical charge, C
λ	=	wavelength, nm
ν_e	=	electron thermal speed, cm $\cdot$ s^{-1}
Σ	=	surface density, cm^{-2}
σ	=	cross section, cm^2
τ	=	pulse width, s

Presented as Paper 0938 at the 40th Aerospace Sciences Meeting and Exhibit, Reno, NV, 14–17 January 2002; received 12 December 2005; revision received 3 May 2006; accepted for publication 5 May 2006.

*Physicist, Photovoltaic and Space Environments Branch; Joel.T.Galofaro@nasa.gov. Member AIAA.
†Senior Scientist. Senior Member AIAA.
‡Senior Research Associate.
§Senior Physicist, Environmental Effects Branch. Senior Member AIAA.

I. Introduction

PREVIOUS studies of the arc initiation process on the solar array surface have shown that the most probable arcing sites were located on the triple junction involving the conductor, dielectric, and plasma [1]. More recently, our own experiments [2] have led us to believe that water vapor is the main causal factor behind the arc initiation process. We hypothesize that the essential component of the expelled plasma cloud is a water vapor, and that the fastest available process to extinguish the discharge arises predominantly from dissociative recombination: ($H_2O^+ + e^- \rightarrow H^* + OH^*$). To validate our hypothesis we obtained and analyzed spectroscopic measurements confirming the presence of hydroxyl (OH) and hydrogen (H) in the arc plasma. Additionally, we also identified a few atomic lines and molecular bands observed in the arc plasma throughout the entire optical range from 260 to 680 nm.

Despite the growing volume of experimental data collected on conductor-dielectric initiated solar array arcs [3–8], only two theoretical models come close to describing the process of arc initiation. The first model is based on the hypothesis that a thin insulating layer on the surface of a negatively charged conductor undergoes electrostatic breakdown when the electric field strength becomes high enough [9]. The second model takes into consideration the formation of a strong electric field in the area of the metal, dielectric, and plasma junctions [10–12]. The estimated average electric field strength in this case is usually a few hundred times below than is typically needed to initiate an arc. Thus, this model demands a field enhancement factor of about 500 which seems improbable. More recently, a new correction to this model has been reported attempting to explain the threshold behavior at the point of arc inception [13]. It is known that gas layers adsorbed on the

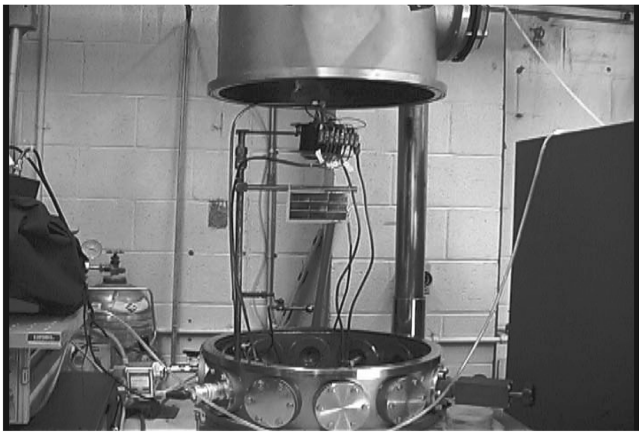

Fig. 1 Bell jar test apparatus used in the arc plasma experiment.

dielectric surface in the area of a triple junction play a significant role in the discharge initiation [14]. The observation of hydroxyl and atomic hydrogen spectral lines confirms the hypothesis that the main constituent of this adsorbed layer is a water vapor. In addition, starting from a desorbed gas ionization mechanism and following dissociative recombination, we derive a relationship between arc current pulse width and capacitance. This rough model predicts the observed dependence of arc pulse width on capacitance with a satisfactory accuracy [15].

II. Experimental Apparatus

The arc initiation experiments were performed in a small bell jar equipped with a mechanical roughing pump, a diffusion pump, and an ionization gauge for measuring tank pressure. A Penning-type plasma discharge source (mounted inside the bell jar) was used as an argon plasma source for the experiments. A Langmuir probe (1.9 cm diameter) with a programmable power supply was used to obtain the needed plasma parameters. Electron temperature ranged between 1.5 and 2 eV, and plasma electron number density ranged between 1.0×10^4 and 8.0×10^5 cm^3. Figure 1 depicts the experimental apparatus just described. Figure 2 shows a close-up view of the solar array sample. The sample consists of three strings wired in parallel. Each string consists of three individual solar cells connected in series.

The capacitor is charged by the bias supply through the resistor, and the shorted array contacts are biased to a large negative potential relative to the walls of the bell jar (see Fig. 3). When an arc occurs both the capacitor and solar array are discharging directly through the plasma. The arc monitor control program detects a change in the trigger state of the oscilloscope and triggers all its four channels at the moment of the discharge initiation.

Figure 4 shows a diagram of the optical setup used for obtaining individual arc spectra. A 1/4 m spectrometer with a 50 μm entrance slit, a 1200 lines/mm grating, and a gated 1024×256 pixel intensified CCD are used for obtaining the optical measurements. The spectrometer is capable of obtaining readings over the wavelength range of 190–920 nm with grating centered on 350 nm.

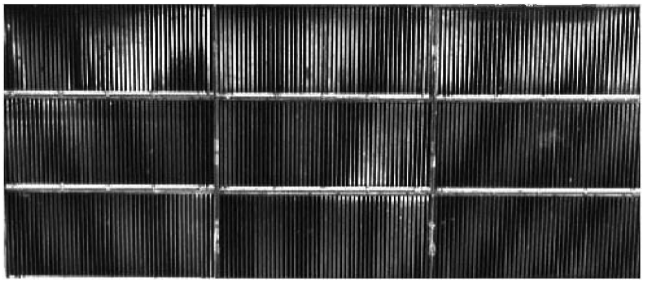

Fig. 2 Snapshot of the small sample used in arc plasma solar array experiments.

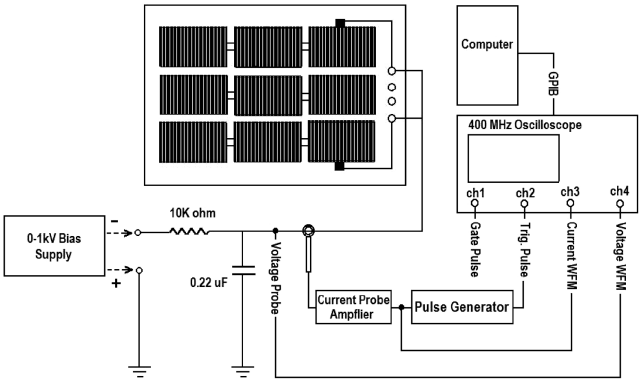

Fig. 3 Experimental setup of arc detection and oscilloscope connections.

A combination of current probe amplifier and oscilloscope provides the needed output trigger for the programmable timing generator (PTG) shown in Fig. 4. The output trigger pulse from the digital storage scope is sent directly to the external trigger input of the PTG. The received input trigger pulse causes the PTG to open the gate of the PI-MAX intensified CCD. A signal sent from the ST-133A controller causes the PI-MAX to capture a single arc spectrum for each detected arc event.

III. Dissociative Recombination

It has been suggested that the main causal factor behind the arc initiation process is a desorbed molecular gas ionization mechanism (specifically, condensed water vapor) at the site of the triple junction. The total number of water molecules ejected into vacuum due to electron impact desorbtion can be estimated as

$$N_W = \Sigma S \tag{1}$$

The dielectric side surface area that is irradiated by energetic electrons on initial stage of the discharge development is roughly 100×100 μm, and a few adsorbed layers of water molecules provide a surface density about 10^{15} cm^2. Thus, the total number of these molecules amounts to about 10^{11}. The degree of ionization of water molecules depends on the electron temperature and varies between 0.01 and 0.1 for generally accepted value of $T_e = 4$–6 eV [16]. The calculations in [16] did not take into account the ionization

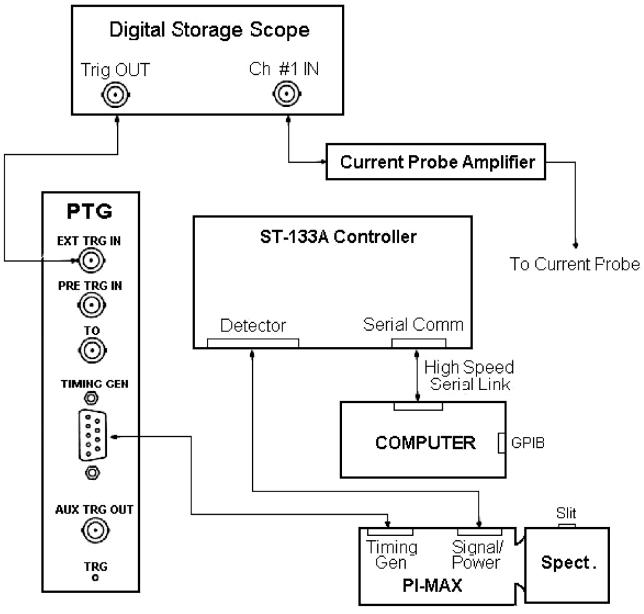

Fig. 4 Diagram showing the experimental setup used for obtaining individual arc spectra.

of water molecules by energetic electrons in the process of electron impact desorbtion; thus, real degree of ionization can be higher. According to [17] a typical vacuum arc supplies about $N_i = 5 \times 10^{15}\,\Delta q$ metal (cathode) ions that are ejected into the chamber during the discharge time interval. For this particular experiment ($C = 0.22\ \mu$F, $U = 200$–300 V), the total number of silver ions is $N_i \gg 10^{11}$. Even though, as it is seen from the preceding estimates, the total number of water ions is 1–2 orders of magnitude lower than the number of metal ions, the influence of water ions on the ionizational balance in the arc plasma can be significant because the rate of dissociative recombination is several orders of magnitude higher than the rate of radiative recombination. One more argument in favor of the dissociative recombination mechanism is comparable intensities of hydrogen and silver spectral lines measured in the current experiment.

The rate of the dissociative recombination $H_2O^+ + e \rightarrow OH^* + H^*$ can be written as

$$\Re = \langle v_e \Sigma \rangle n_e^2 = \gamma n_e^2 \tag{2}$$

The braces in the preceding equation indicate the expectation value of the product of the thermal velocity and the cross section. We disregarded the contribution of metal ions in the total charged particle number density assuming the quasi neutrality of arc plasma in the form $n_e = n(H_2O^+)$. The molecular-ion recombination constant can be presented in the simple form [18]

$$\gamma \gg \frac{10^{-7}}{\sqrt{T_e}} \tag{3}$$

Disregarding the collisional ionization in a cold arc plasma we can write the equation for electron number density:

$$\frac{dn_e}{dt} = -\gamma n_e^2 \tag{4}$$

If we suggest that cooling of the electron gas due to plasma expansion is much slower that recombination we can write the solution of Eq. (4) with the appropriate initial condition at $t = 0$ in the following form:

$$n_e(t) = \frac{n_{eo}}{1 + n_{eo}\gamma t} \tag{5}$$

The electric current $I(t)$ to the surface of a hemispheric arc plasma cloud of radius $R(t)$ (1–2 cm) at the dielectric-conductor junction is simply

$$I(t) = 2\pi R(t)^2 n_e(t) e V_e \tag{6}$$

The velocity of plasma cloud expansion can be estimated as

$$V_p = \sqrt{\frac{2kT_e}{Am_p}} \tag{7}$$

For typical electron temperatures $T_e = 4$–6 eV this velocity reaches 7–10 km/s for water ions ($A = 18$). The estimated value of the velocity of metal plasma expansion is a few times lower than measured one (see [17]). It means that our further calculations must be considered as rough estimates, which reveal basic relations between measured arc parameters.

The radius of the plasma cloud is given by

$$R(t) = V_p t \tag{8}$$

Substituting Eqs. (5), (7), and (8) into Eq. (6) yields the electric current

$$I(t) = 4\pi \frac{ekT_e}{Am_p} V_e \frac{n_{eo} t^2}{1 + n_{eo}\gamma t} \tag{9}$$

The net electric charge carried our from the capacitor by this current is

$$CU = \int_0^\tau I(t)\,dt \tag{10}$$

Substituting Eq. (9) into integral and taking into account that $n_{eo}\gamma t \gg 1$ we obtain

$$\tau = \left[\frac{Am_p\gamma}{2\pi k T_e e V_e}\right]^{1/2} (CU)^{1/2} \tag{11}$$

This relation between arc current pulse width and capacitance was obtained in a slightly different form in [15]. The dependence of pulse width on capacitance can be easily verified in the experiment. By the compilation of the results of six different experiments it was found that $\ell n\,\tau / \ell n\,C = 0.627 - 0.016$ within the wide range of capacitance values (10^{-3}–$10^3\ \mu$F) [19,20]. In the narrow range of capacitances (0.04–0.065 μF) the slope was determined as $0.5 - 0.05$ [15]. Later, the dependence $\tau(C)$ was measured within the interval of capacitances of 5×10^{-3}–$3 \times 10^{-2}\ \mu$F, and significant deviation from the square root dependence was found [21]. Thus, one can conclude that the simple model of a discharge development based solely on the process of dissociative recombination of water molecular ions can pretend on just qualitative description of real processes in the arc plasma. However, the presence of water molecules in the arc plasma was confirmed by mass spectrometry, and thermal outgassing of the sample resulted in a sharp decrease in arc rate [21]. These two series of observations stimulate further experimental investigation that can be performed by the measurements of emission spectra of the arc plasma.

IV. Optical Spectroscopy

All arc spectra shown in this paper have been obtained using an intensified CCD array cooled to $-20°$C to reduce the internal noise. Twenty rows of vertical pixels ($120 + 20$ vertical pixels out of a possible 256 pixels and 1024 horizontal pixels out of a 256×1024 array) were used to keep the signal to noise ratio within acceptable limits. Each spectrum shown covers a wavelength range of about 100 nm divided by 1024 pixels. Spectrometer calibration was performed using standard Oriel 6030 and 6031 lamps. The spectral resolution of employed optical system was determined as of 0.109 nm/pixel. A minimum of two spectral lines with known wavelengths and the corresponding pixel numbers are needed to manually calibrate the spectrometer within the chosen range. For those instances where only one known line was registered, the linear interpolation was used:

$$\lambda_c = \lambda_k + 0.109(P_c - P_k)$$

Four to six individual spectra are gathered at each wavelength setting to insure that the features present were repeatable and not merely artifacts of the measurement process. Measurements were obtained at the central wavelength starting at 260 nm. The entire optical spectra from 260 to 680 nm in wavelength were systematically scanned in 50 nm increments.

The distance between the spectrometer and the solar array was set to 16 cm. The small chamber size and random arc site locations (from one side of the array to another) caused shifts of ± 4 nm in measured wavelengths. To correct this problem the array sample was masked down to the area of one cell leaving one pair of interconnects exposed to the plasma.

One example of spectrum is shown in Fig. 5. Atomic and molecular spectral lines (bands) were identified according to [22–24]. It is seen in Fig. 5 that the most intensive spectral lines belong to silver atoms and ions. This observation supports the general idea of a commonality between vacuum arcs and discharges on triple junction: in both cases the negatively biased electrode erosion is caused by arc current pulses.

The wide band structure at 302–309 nm is well known as the hydroxyl molecular band. The OH band is observable in emission in arcs where water vapor is present [24]. The most intensive line in the OH band occurs at 306.3 nm (Fig. 6). The low observed line intensity can be explained by a significant absorption of UV light propagating

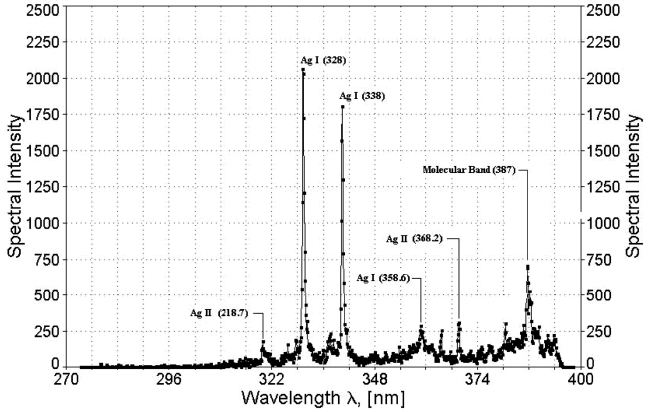

Fig. 5 Typical atomic lines and molecular band in emission spectrum of arc plasma.

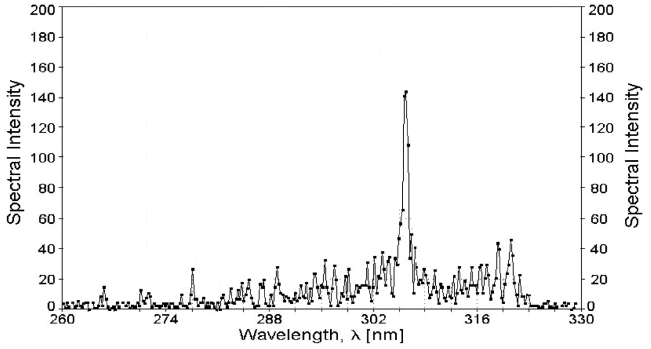

Fig. 6 Hydroxyl emission spectrum. Spectrometer set at the central line of 270 nm.

through a glass window installed in the bell jar. The cutoff wavelength for a glass is approximately 350 nm, and this translates to a six times decrease in intensity at 306.3 nm.

Figure 7 shows a molecular band at 387 nm, two wide bands at 434 nm and 472 nm, a molecular band for SiH at 387 nm, a wide band for CH at approximately 432 nm, and molecular band SiN at 472 nm [24] The SiH (387 nm) band is often present in silicon arcs in hydrogen (silicon may come from solar cell and/or adhesive). The CH molecular band often occurs in electrical discharges where carbon molecules and hydrogen molecules are present. Two atomic lines at approximately 408.7 nm and 415.8 nm are also shown in Fig. 7. Harrison [23] lists one of two possible lines at 408.7 nm as either ion Fe (408.710 nm) or O^+ (O II at 408.714 nm), but is beyond the spectral resolution of our equipment to say which is correct. An atomic line for iron, Fe I at 415.879 nm is also identified. We may

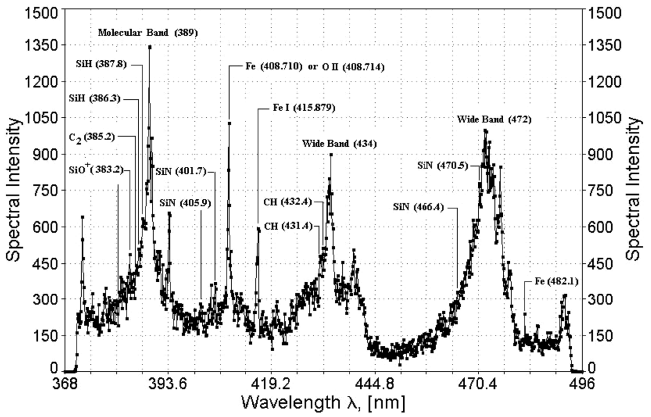

Fig. 7 Variety of atomic and molecular emission spectral patterns from single plasma arc.

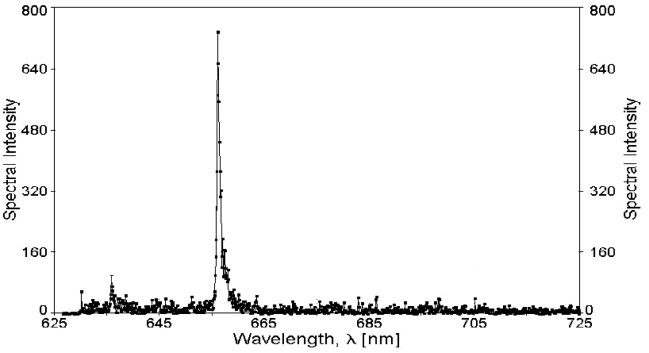

Fig. 8 One example of H-α spectral line.

suggest that atomic lines of iron were observed due to the erosion of the invar electrodes.

The most important observation is a strong atomic hydrogen line (H-α, 656.3 nm). It is seen in Fig. 8 that the intensity of this line is only three times lower than the intensity of atomic silver line (328 nm, Fig. 5). Corresponding transitional probability for a hydrogen atom is approximately two times lower than for a silver atom; thus, one can conclude that both atomic number densities are close to each other. Finally, a strong H-β, line at 486 nm (not shown) was also observed with an intensity of 500.

V. Conclusions

It is hypothesized that a desorbed gas ionization process occurring at the triple junction on a solar array surface is responsible for the onset of arc initiation. We suggest a simple dissociative recombination mechanism that predicts a simple square root dependence of the arc current pulse width on bias voltage and capacitance. Series of tests demonstrated at least a qualitative agreement with our model whereas exact quantitative theoretical analysis needs to be performed for a validation of the hypothesis.

The observations of arc optical spectra lend credence to the suggested molecular gas ionization process as an essential part of the arc initiation mechanism. The presence of hydroxyl in arc plasma is an indicator of a dissociation of water molecular ions. High-intensity hydrogen spectral lines observed in arc plasma emission spectra confirm the presence of water molecular ions in this plasma. Moreover, comparison of hydrogen and metal (silver) line intensities results in a conclusion about comparable number densities of these ions in the arc plasma. Outgassing solar array surface by thermal cycling and pumping out the residual gases resulted in a sharp decrease in arc rate on a large sample [21,25]. This is undoubtedly one more strong argument in favor of a suggestion about a significant role of adsorbed water in arc initiation process.

The obtained results seem to be important for the prevention of electrostatic discharges on spacecraft surfaces. Really, most conventional arrays are backed with stiff supporting structures composed of honeycomb aluminum matrix filled with either graphite or fiberglass. Graphite and fiberglass are both porous materials able to adsorb water vapor. Thus, an array on a spacecraft launched at sea level into low earth orbit contains water vapor, and it is outgassing continuously due to solar heating and space vacuum. The rate of outgassing is higher during a few initial orbits, and this leads to a high probability of arcing on solar array. If a whole structure would be degassed in vacuum chamber and properly packed before the deployment in orbit, the probability of a discharge diminished significantly.

References

[1] Hastings, D. E. "A Review of Spacecraft/Plasma Interaction and Effects on Space Systems," *Journal of Geophysical Research*, Vol. 100, No. A8, 1995, pp. 14,457–14,483.

[2] Galofaro, J. T., Vayner, B. V., Ferguson, D. C., and Degroot, W. A., "A Desorbed Gas Molecular Ionization Mechanism for Arcing Onset in

Solar Arrays Immersed in a Low-Density Plasma," AIAA Paper 2002-2262, June 2002.
[3] Stevens, N. J., "Interactions Between Spacecraft and the Charge-Particle Environment," *Proceedings of Spacecraft Charging Technology Conference*, CP-2071, NASA, 1978, pp. 268–294.
[4] Ferguson, D. C., "Solar Array Arcing in Plasmas," NASA CP-3059, 1989, p. 509.
[5] Hastings, D. E., Weyl, G., and Kaufman, D., "Threshold Voltage for Arcing on Negatively Biased Solar Arrays," *Journal of Spacecraft and Rockets*, Vol. 27, No. 5, 1990, pp. 539–544.
[6] Vaughn, J. A., Carruth, M. R., Jr., Katz, I., Mandell, M. J., and Jongeward, G. A., "Electrical Breakdown Currents on Large Spacecraft in Low Earth Orbit," *Journal of Spacecraft and Rockets*, Vol. 31, No. 1, 1994, pp. 54–59.
[7] De la Cruz, C. P., Hastings, D. E., Ferguson, D. C., and Hillard, D. B., "Data Analysis and Model Comparison for Solar Array Module Plasma Interactions Experiment," *Journal of Spacecraft and Rockets*, Vol. 33, No. 3, 1996, pp. 438–446.
[8] Koons, H. C., "Summary of Environmentally Induced Discharges on the P78-2 (SCATHA) Satellite," *Journal of Spacecraft and Rockets*, Vol. 20, No. 5, 1983, pp. 425–431.
[9] Parks, E. D., Jongeward, G., Katz, I., and Davis, V. A., "Threshold-Determining Mechanisms for Discharges in High Voltage Solar Arrays," *Journal of Spacecraft and Rockets*, Vol. 24, No. 4, 1987, pp. 367–371.
[10] Cho, M., and Hastings, D. E., "Computer Simulation on High-Voltage Solar Array Arcing Onset," *Journal of Spacecraft and Rockets*, Vol. 30, No. 2, 1993, pp. 189–205.
[11] Mong, R., and Hastings, D. E., "Arc Mitigation on High Voltage Solar Arrays," *Journal of Spacecraft and Rockets*, Vol. 31, No. 4, 1994, pp. 684–690.
[12] Upschulte, B. L., Marinelli, W. J., Carleton, K. L., Weyl, G., Aifer, E., and Hastings, D. E., "Arcing on Negatively Biased Solar Cells in a Plasma Environment," *Journal of Spacecraft and Rockets*, Vol. 31, No. 3, 1994, pp. 493–501.
[13] Katz, I., Davis, V. A., and Snyder, D. B., "Mitigation Techniques for Spacecraft Charging Induced Arcing on Solar Arrays," AIAA Paper 99-0215, Jan. 1999.
[14] Anderson, R. A., and Brainard, J. P., "Mechanism of Pulsed Surface Flashover Involving Electron-Simulated Desorption," *Journal of Applied Physics*, Vol. 51, No. 3, 1979, pp. 1414–1421.
[15] Vayner, B. V., Galofaro, J., and Ferguson, D., "Arc Inception on a Solar Array Immersed in a Low-Density Plasma," NASA TM-2001-211070, 2001.
[16] Vayner, B., Galofaro, J., Ferguson, D., and Degroot, W., "Electrostatic Discharge Inception on a High-Voltage Solar Array," AIAA Paper 2002-0631, Jan. 2002.
[17] Anders, A., "Ion Charge State Distribution of Vacuum Arc Plasmas: The Origin of Species," *Physical Review E (Statistical Physics, Plasmas, Fluids, and Related Interdisciplinary Topics)*, Vol. 55, No. 1, 1997, pp. 969–981.
[18] Kaplan, S. A., and Pikel'ner, S. B., *Physics of Interstellar Medium*, Nauka, Moscow, 1979, p. 376.
[19] Snyder, D. B., and Tyree, E., "The Effect of Plasma on Solar Cell Array Characteristics," NASA TM 86887, 1984, pp. 1–6.
[20] Snyder, D. B., "Characteristics of Arc Currents on a Solar Cell Array in a Plasma," *IEEE Transactions on Nuclear Science*, Vol. 31, No. 4, 1984, pp. 1584–1587.
[21] Vayner, B., Galofaro, J., and Ferguson, D., "Interactions of High-Voltage Solar Arrays with Their Plasma Environment: Ground Tests," *Journal of Spacecraft and Rockets*, Vol. 41, No. 6, 2004, pp. 1041–1050.
[22] Wiese, W. L., Smith, M. W., and Glennon, B. M., *Atomic Transition Probabilities: A Critical Data Compilation*, National Bureau of Standards, U.S. Department of Commerce, 1966.
[23] Harrison, G. R. (ed.), *Masssachusetts Institute of Technology Wavelength Tables*, MIT Press, Cambridge, MA, 1960.
[24] Pearce, R. W. B., and Gaydon, A. G., *The Identification of Molecular Spectra*, 3rd ed., Chapman & Hall, London, 1963.
[25] Vayner, B., Galofaro, J., and Ferguson, D., "Interactions of High-Voltage Solar Arrays with Their Plasma Environment: Physical Processes," *Journal of Spacecraft and Rockets*, Vol. 41, No. 6, 2004, pp. 1031–1040.

I. Boyd
Associate Editor